Supplemental Figures

Supplemental Figure 1

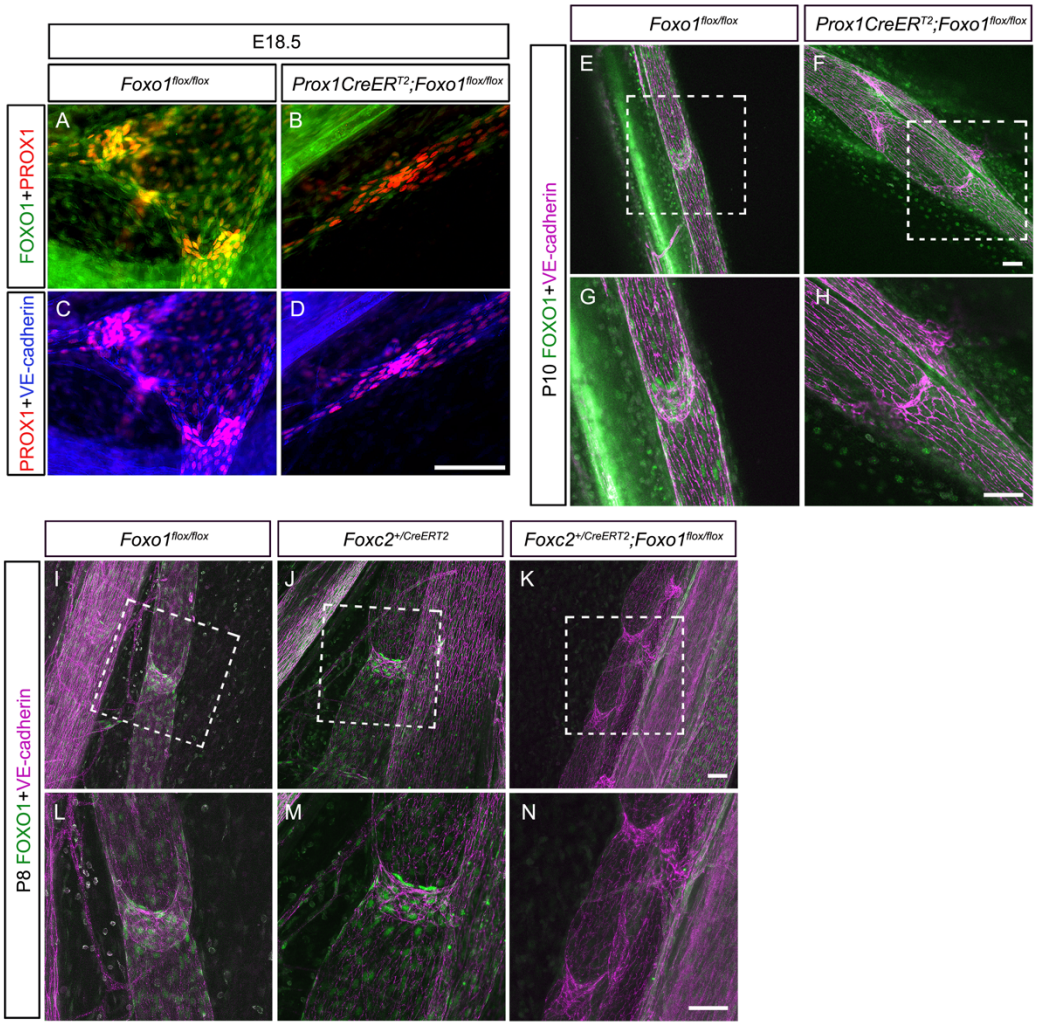

Supplemental Figure 1. Tamoxifen injection completely abolishes the expression of FOXO1 in the embryonic and postnatal lymphatic vessels. (A-D) Whole-mount immunostaining of mesenteries collected from E18.5 control and *Foxo1*$^{LEC\text{-}KO}$ with FOXO1 (green), PROX1 (red), and VE-cadherin (blue). (E-H) Whole-mount immunostaining of mesenteries collected from P10 control and *Foxo1*$^{LEC\text{-}KO}$ with FOXO1 (green) and VE-cadherin (purple). (I-N) Whole-mount immunostaining of mesenteries collected from P8 control, *Foxc2*$^{+/CreERT2}$, and *Foxc2*$^{+/CreERT2}$;*Foxo1*$^{flox/flox}$ with FOXO1 (green) and VE-cadherin (purple). G, H, L, M, and N are

the higher magnification images of the white squared areas in E, F, I, J, and K. Scale bars are 200μm in (D) and 50μm in (F, H, K, and N). Mesenteries from four controls and four knockouts were analyzed.

Supplemental Figure 2

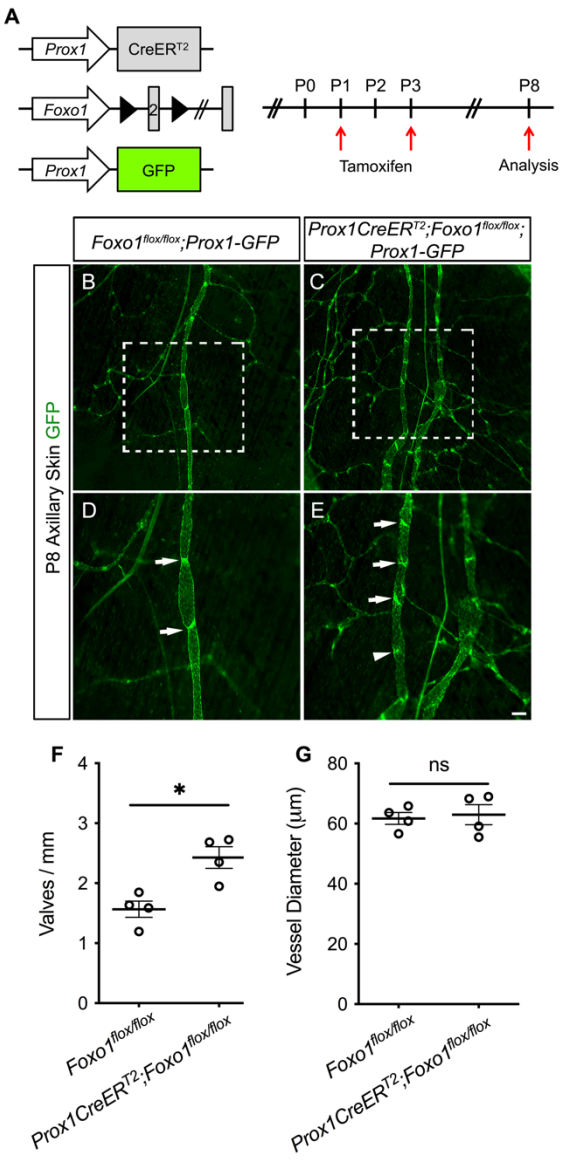

Supplemental Figure 2. Postnatal deletion of *Foxo1* leads to additional valve growth in the axillary lymphatic vessels. (A) Tamoxifen injection procedure for postnatal deletion of *Foxo1*. (B-E) Fluorescence imaging of the morphology of the axillary lymphatic vessels indicated by GFP expression from P8. The valves are indicated by white arrows and the valve-forming area is indicated by a white arrowhead in the *Foxo1*$^{LEC\text{-}KO}$ axillary vessel. Scale bar is 100μm in (E). (F) Valves per millimeter from each mesentery. (G) The average diameter of the axillary lymphatic

vessel from each animal. Four controls and four knockouts were analyzed. *$p<0.05$ and ns=not significant calculated by unpaired Student's t-test. All values are means ± SEM.

Supplemental Figure 3

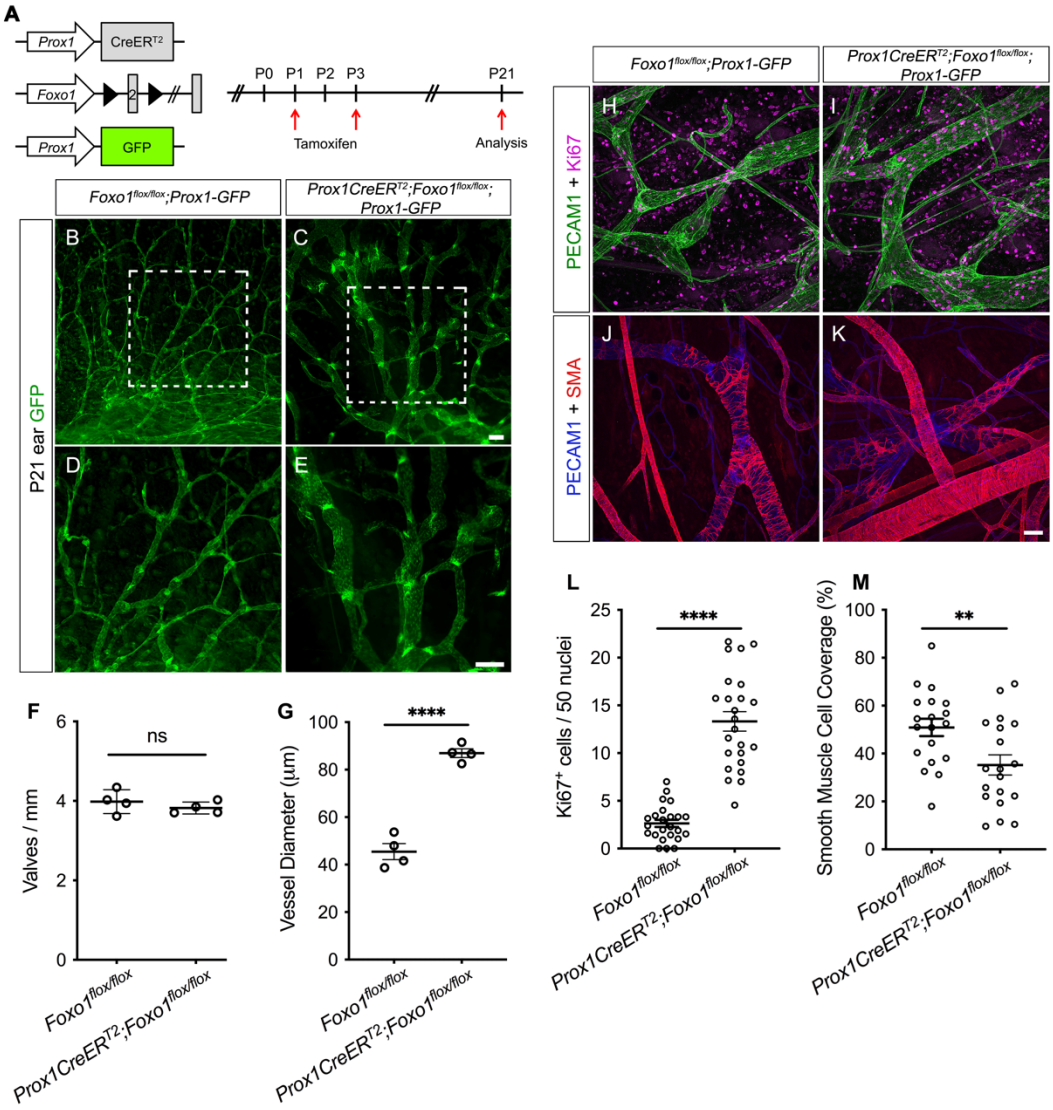

Supplemental Figure 3. Ablation of *Foxo1* causes dilation and reduction of smooth muscle cell coverage in the ear lymphatic vessels. (A) Tamoxifen injection procedure for postnatal deletion of *Foxo1*. (B-E) Fluorescence imaging of the morphology of the ear lymphatic vessels indicated by GFP expression from P21. (F) Valves per millimeter from each animal. (G) The average diameter of the ear collecting lymphatic vessels. All values are means ± SEM. ****p<0.0001, ns=not significant, calculated by unpaired Student's t-test. Four controls and four knockouts were used in the analysis. (H and I) Whole-mount immunostaining of P21 ears with PECAM1 (green) and

Ki67 (purple). (J and K) Whole-mount immunostaining of ears collected from P21 control and *Foxo1*$^{LEC\text{-}KO}$ with PECAM1 (blue) and SMA (red). Scale bars are 200μm in (C and E), 50μm in (K). (L) Quantification of Ki67 positive cells in the ear collecting lymphatic vessels. (M) Quantification of smooth muscle cell coverage in the ear collecting lymphatic vessels. All values are means ± SEM. ****$p<0.0001$, **$p<0.01$, calculated by unpaired Student's t-test. Four controls and four knockouts were used in the analysis.

Supplemental Figure 4

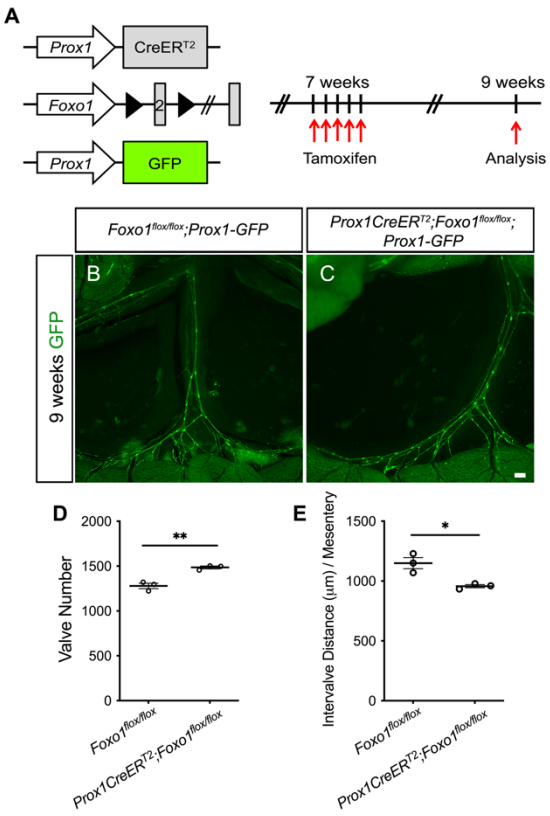

Supplemental Figure 4. Loss of *Foxo1* in adult mice results in increased formation of lymphatic valves. (A) Tamoxifen injection procedure for deletion of *Foxo1* in the adult mice. (B and C) Fluorescence imaging of the morphology of the mesenteric lymphatic vasculature indicated by GFP expression from 9-week old mice. (D) Total number of mature valves from each mesentery. (E) The distance between two adjacent valves from each mesentery. Scale bar is 500μm. All values are means ± SEM. Three controls and three knockouts were used in the analysis. **p<0.01 and *p<0.05, calculated by unpaired Student's t-test.

Supplemental Figure 5

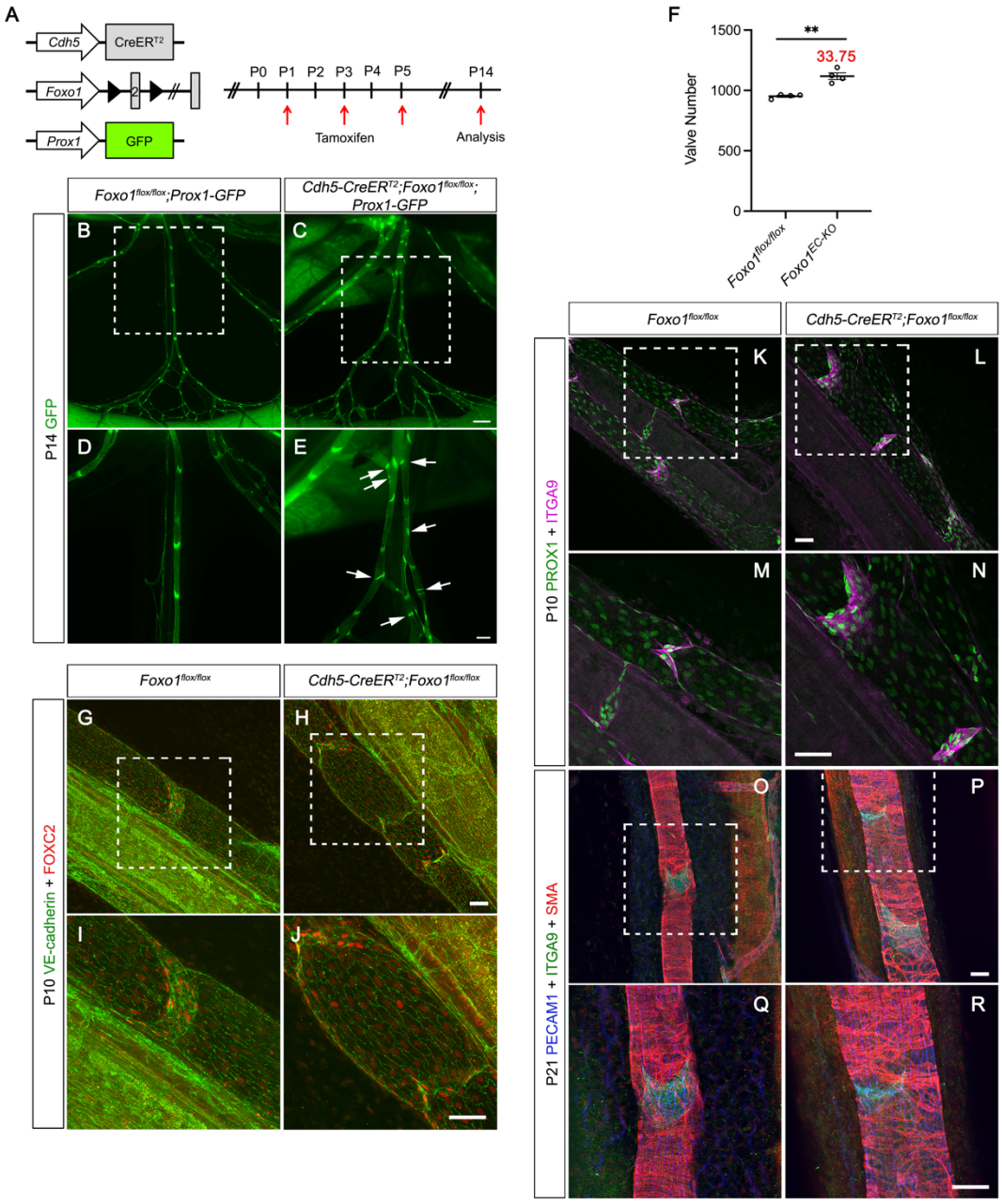

Supplemental Figure 5. Deletion of *Foxo1* using the pan-endothelial *Cdh5-CreER^{T2}* leads to additional valve growth in the lymphatic vasculature. (A) Tamoxifen injection procedure for postnatal deletion of *Foxo1*. (B-E) Fluorescence imaging of the morphology of the mesenteric

lymphatic vasculature indicated by GFP expression from P14. The *Cdh5-CreER^{T2};Foxo1$^{flox/flox}$* mesentery has many valve initiation and elongation areas (white arrows). D and E are the higher magnification images of the white squared areas in B and C. (F) Total number of mature valves from each mesentery. The red number is the average number of immature valves. All values are means ± SEM. Four controls and four knockouts were used in the analysis. **p<0.01, calculated by unpaired Student's t-test. (G-N) Whole-mount immunostaining of mesenteries collected from P10 control and *Cdh5-CreER^{T2};Foxo1$^{flox/flox}$* with VE-cadherin (green), FOXC2 (red), PROX1 (green), and ITGA9 (purple). I, J, M, and N are the higher magnification images of the white squared areas in G, H, K, and L. (O-R) Whole-mount immunostaining of mesenteries collected from P21 control and *Cdh5-CreER^{T2};Foxo1$^{flox/flox}$* with PECAM1 (blue), ITGA9 (green), and SMA (red). Q and R are the higher magnification images of the white squared areas in O and P. Scale bars are 500μm in (C), 200μm in (E) and 50μm in (H, J, L, N, P, and R). Four controls and four knockouts were used in the analysis.

Supplemental Figure 6

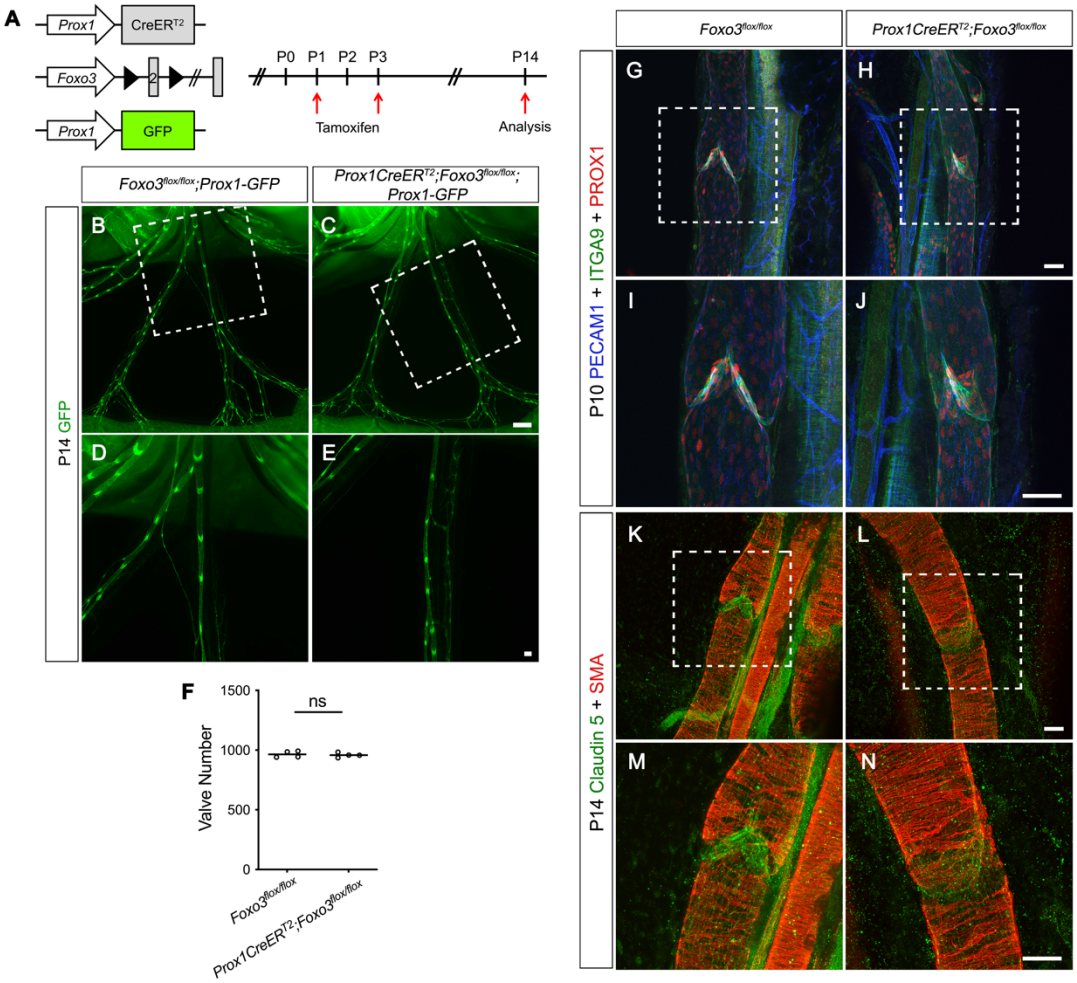

Supplemental Figure 6. Postnatal deletion of *Foxo3* in the lymphatic vasculature does not induce additional valve growth. (A) Tamoxifen injection procedure for postnatal deletion of *Foxo3*. (B-E) Fluorescence imaging of the morphology of the mesenteric lymphatic vasculature indicated by GFP expression from P14. D and E are the higher magnification images of the white squared areas in B and C. (F) Total number of valves from each mesentery. All values are means ± SEM. Four controls and four knockouts were used in the analysis. ns=not significant, calculated by unpaired Student's t-test. (G-J) Whole-mount immunostaining of mesenteries collected from P10

control and *Foxo3*$^{LEC\text{-}KO}$ with PECAM1 (blue), ITGA9 (green), and PROX1 (red). (K-N) Whole-mount immunostaining of mesenteries collected from P14 control and *Foxo3*$^{LEC\text{-}KO}$ with Claudin 5 (green) and SMA (red). I, J, M, and N are the higher magnification images of the white squared areas in G, H, K, and L. Scale bars are 500μm in (C), 100μm in (E), and 50μm in (H, J, L, and N). Three controls and three knockouts were used in the analysis.

Supplemental Figure 7

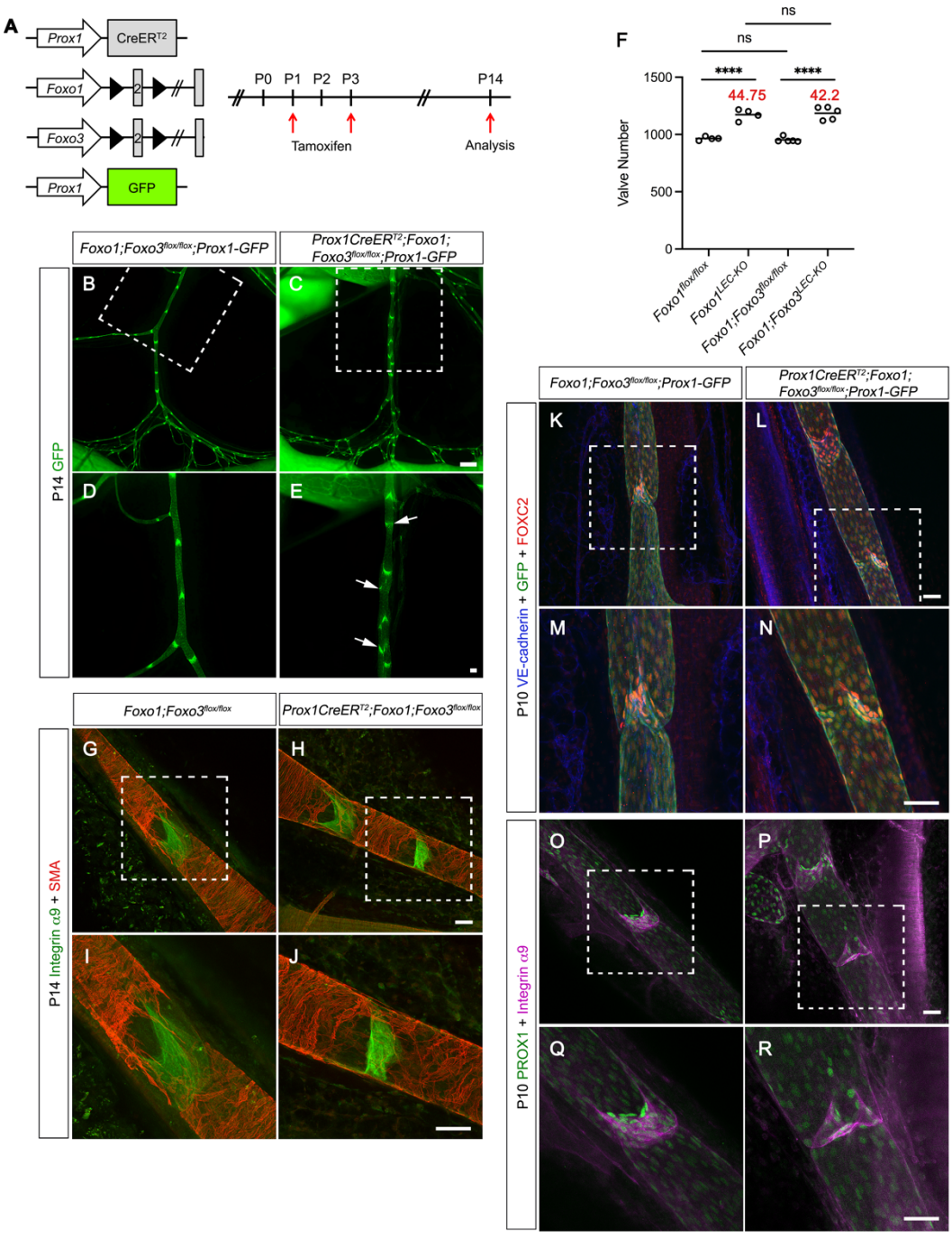

Supplemental Figure 7. The growth of new valves upon the loss of *Foxo1* does not require Foxo3 activity in the postnatal lymphatic vasculature. (A) Tamoxifen injection procedure for postnatal

deletion of *Foxo1* and *Foxo3*. (B-E) Fluorescence imaging of the morphology of the mesenteric lymphatic vasculature indicated by GFP expression from P14. D and E are the higher magnification images of the white squared areas in B and C. (F) Total number of mature valves from each mesentery. The red numbers are the average number of immature valves. (G-J) Whole-mount immunostaining of mesenteries collected from P14 control and *Foxo1*;*Foxo3*$^{LEC\text{-}KO}$ with ITGA9 (green) and SMA (red). (K-R) Whole-mount immunostaining of mesenteries collected from P10 control and *Foxo1*;*Foxo3*$^{LEC\text{-}KO}$ with PECAM1 (blue), GFP (green), FOXC2 (red), PROX1 (green), and ITGA9 (purple). I, J, M, N, Q, and R are the higher magnification images of the white squared areas in G, H, K, L, O, and P. All values are means ± SEM. 4-5 controls and 4-5 knockouts were used in the analysis. One-way ANOVA was performed with Tukey's multiple comparisons test (****$p<0.0001$ and ns=not significant). Scale bars are 500μm in (C), 100μm in (E), and 50μm in (H, J, L, N, P, and R).

Supplement Figure 8

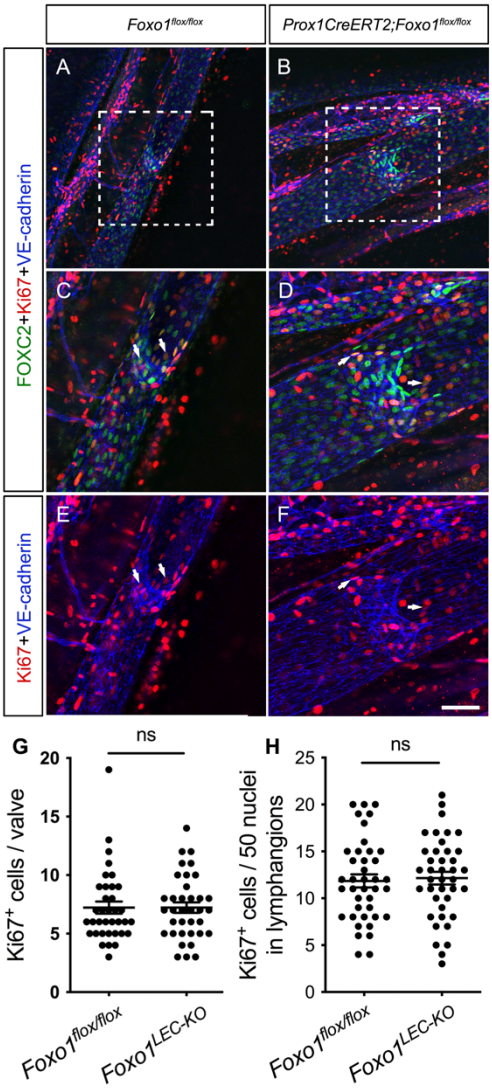

Supplemental Figure 8. Loss of *Foxo1* does not affect proliferation in postnatal vessels. (A-F) Whole-mount immunostaining of mesenteries collected from P10 control and *Foxo1*$^{LEC\text{-}KO}$ with FOXC2 (green), Ki67 (red), and VE-cadherin (blue) when tamoxifen was injected at P1P3. C-D are the higher magnification images of the white squared areas in A and B, whereas E-F are the same without FOXC2 overlaid. White arrows indicate the examples for Ki67/FOXC2 double positive cells in the valves and lymphangions. Scale bar is 50μm. (G and H) Quantification of Ki67 positive cells in the valves and in the lymphangions. All values are means ± SEM. Four controls

and four knockout mesenteries were used in the analysis. Each dot represents one vessel or one valve from each mesentery. ns=not significant, calculated by unpaired Student's t-test.

Supplemental Methods

Ex vivo Analysis of Lymphatic Vasculature and Lymphatic Valve Quantification

The results for “valves per mm” were generated as “total valve number / total vessel length”. The total length of each collecting vessels (including the large collecting vessels and those thinner branched pre-collecting vessels located close to the intestinal wall) was measured using Fiji (NIH ImageJ) software. The total number of valves located in each collecting vessel was counted using a hand tally counter. Four control and four knockout animals were used for eight measurements from each mesentery. The selection was consistent between vessels and mesenteries.

The number of branches was the average number of the branches from eight large collecting vessels in each mesentery, which was counted using a hand tally counter. The branches are located in the thinner pre-collecting vessels close to the intestinal wall. Four control and four knockout animals were used.

The intervalve distance between two adjacent valves in the large collecting vessels of adult mice was measured using Fiji software. The valves are located in the segment of each large collecting vessel between the lymph node and the first branch of each vessel. Four control and four knockout animals were used for thirty measurements from each mesentery.

Lymphatic vessel diameter was measured using Fiji software. For mesenteric lymphatic vessels, three measurements were performed in the segment of each large collecting vessel between the lymph node and the first branch of the vessel in the mesentery to obtain the average diameter of each large collecting vessel. Six large collecting vessels in each mesentery were used for the analysis. For axillary and ear lymphatic vessels, three measurements were performed in each collecting lymphatic vessel to obtain the average diameter of the vessel. Three to four collecting lymphatic vessels in each ear were used for the analysis. Four control and four knockout animals were analyzed for each time point per tissue type. Control and knockout littermates were generated in pairs from four independent litters for all of the analyses above.

Quantification of Cell Proliferation in the Lymphatic Vessels

Mesenteries at P10 and ears at P21 from four controls and four knockout mice were collected and immunostained with FOXC2, Ki67, and VE-cadherin for the mesenteries and SMA, Ki67, and PECAM1 for the ears following the whole-mount immunostaining procedure. The number of Ki67 positive cells in ten collecting lymphatic vessels and nine valves from each mesentery, and three collecting lymphatic vessels from each ear was counted after confocal imaging. Four controls and four knockouts were analyzed for each tissue type.

Quantification of Smooth Muscle Cell Coverage

Ears at P21 from four controls and four knockout mice were collected and immunostained with SMA for smooth muscle cells and GFP for *Prox1-GFP* tissues following the whole-mount immunostaining procedure. After confocal imaging, the smooth muscle cell coverage was measured using Fiji software. Both the image of SMA and GFP were acquired. The procedure was to 1) draw multiple ROIs precisely to trace the collecting lymphatic vessels avoiding the blood vessels using “ROI manager”; 2) use the “Threshold” tool to set the intensity of the vessels using GFP signal and the intensity of the smooth muscle cells using SMA signal; 3) after applying the threshold, use “Invert” tool to invert the images; 4) use “Measure” tool in the “ROI manager” to obtain the information of “area” and “area fraction” of both sets of images with the “limit to threshold” setting in the “set measurements” tool; 5) derive the final areas of both the smooth muscle cells and the vessels by multiplying “area” by “area fraction”; 6) obtain the percentage of smooth muscle cell coverage by dividing smooth muscle cell area by vessel area.

Whole-Mount Immunostaining Procedure

The intestine and associated mesentery was excised and pinned onto a Sylgard 184 cushion. The tissues were fixed overnight in 1% paraformaldehyde for embryonic tissues and 2% paraformaldehyde for postnatal tissues at 4^{o}C on an orbital shaker (Belly Dancer, IBI Scientific). The next day, tissues were washed with PBS three times 10 minutes each. To start whole-mount immunostaining, tissues were permeabilized with PBS + 0.3% Triton X-100 (PBST) for one hour

and blocked with 3% donkey serum in PBST for two hours at 4°C on the orbital shaker. Primary antibodies were prepared in PBST, added to the tissue, and incubated overnight at 4°C on the orbital shaker. The next day, tissues were washed five times for 15 minutes each with PBST at 4°C on the orbital shaker to remove primary antibodies. Secondary and conjugated antibodies were prepared in PBST, added to the tissues, and incubated at room temperature for 1.5 hours on an orbital shaker (Belly Button, IBI Scientific). Tissues were then washed five times 15 minutes each with PBST at 4°C on the orbital shaker. To provide nuclear contrast, DAPI was dissolved in PBS, added to the tissues, and incubated at room temperature for 5 minutes, followed by a wash in PBS for 5 minutes. Tissues were then mounted on glass slides (Superfrost Plus Microscope slides, Fisherbrand) with ProLong Diamond Antifade Mountant containing DAPI (Invitrogen). Four control and four knockout tissues were used in the whole-mount immunostaining. Immunostained tissues were imaged on an inverted fluorescence microscope (Axio Observer Z1, Zeiss) or a Leica SP8 confocal microscope. Images were acquired with Zen 2 Pro software and Leica Application Suite X software. Figures were created using Image J and Adobe Photoshop.

Antibodies

Primary antibodies used for immunostaining were as follows: rabbit anti-PROX1 (Abcam, ab101851), goat anti-human PROX1 (R&D Systems, AF2727), sheep anti-mouse FOXC2 (R&D Systems, AF6989), rat anti-mouse VE-cadherin (BD Pharmingen, 550548), rat anti-mouse CD31 (BD Pharmingen, 550274), rabbit anti-FOXO1 (Cell Signaling, 2880), rabbit anti-GATA2 (Novus Biologicals, NBP1-82581), rabbit anti-β-catenin (Millipore, 06-734), goat anti-mouse Integrin α9 (R&D Systems, AF3827), goat anti-mouse KLF4 (R&D Systems, AF3158), rabbit anti-Claudin 5 (ThermoFisher, 34-1600), rabbit anti-Ki67 (Abcam, ab15580), Alexa488-conjugated anti-GFP (Life Technologies, A21311), and Cy3-conjugated monoclonal anti-α-SMA (Sigma-Aldrich, C6198). The following secondary antibodies were used: Alexa Fluor 488 Donkey Anti-Rabbit IgG (H+L) (Invitrogen, A-21206), Alexa Fluor 488 Donkey Anti-Goat IgG (H+L) (Invitrogen, A-11055), Alexa Fluor 488 Donkey Anti-Sheep IgG (H+L) (Invitrogen, A-11015), Alexa Fluor 488 Donkey

Anti-Rat IgG (H+L) (Invitrogen, A-21208), Alexa Fluor 594 Donkey Anti-Rabbit IgG (H+L) (Invitrogen, A-21207), Alexa Fluor 594 Donkey Anti-Goat IgG (H+L) (Invitrogen, A-11058), Alexa Fluor 594 Donkey Anti-Sheep IgG (H+L) (Invitrogen, A-11016), Alexa Fluor 594 Donkey Anti-Rat IgG (H+L) (Invitrogen, A-21209), Alexa Fluor 647 Donkey Anti-Rabbit IgG (H+L) (Invitrogen, A-31573), and Alexa Fluor 647 Donkey Anti-Goat IgG (H+L) (Invitrogen, A-21447) were purchased from Life Technologies. Alexa Fluor 647 Donkey Anti-Rat IgG (H+L) (712-605-153) was purchased from Jackson ImmunoResearch Laboratories.

Primary antibodies used for western blot were as follows: mouse anti-FOXC2 (Santa Cruz, sc-515234), goat anti-GATA2 (R&D Systems, AF2046), rabbit anti-KLF4 (Novus Biologicals, NBP2-24749), rabbit anti-FOXO1 (Cell Signaling, 2880), rabbit anti-Phospho-FOXO1 (Ser319) (Cell Signaling, 2486S), rabbit anti-AKT (Cell Signaling, 4691S), rabbit anti-Phospho-AKT (Ser473) (Cell Signaling, 4060S), mouse anti- β-Actin (Cell Signaling, 3700). The following secondary antibodies were used: Donkey anti-Goat IgG (H+L) Cross-Adsorbed Secondary Antibody, HRP (Invitrogen, A16005), Donkey anti-Rabbit IgG (H+L) Highly Cross-Adsorbed Secondary Antibody, HRP (Invitrogen, A16035), Donkey anti-Mouse IgG (H+L) Highly Cross-Adsorbed Secondary Antibody, HRP (Invitrogen, A16017).

RNA isolation and Quantitative Real-time PCR

Total RNA was isolated from cells using RNeasy Plus Mini Kit (Qiagen) according to the manufacturer's protocol. cDNA was synthesized from total RNA using the Advantage® RT-for-PCR Kit (Takara) following the manufacturer's instructions. Quantitative PCR (qPCR) was performed using TaqMan® probes (Applied Biosystems, ThermoFisher) in a QuantStudio 3 realtime system (Applied Biosystems). The threshold cycle (Ct) value for each gene was normalized to the Ct value for GAPDH.

Western Blot

Total protein was harvested using RIPA buffer (Pierce™, ThermoFisher). The concentrations of the protein were measured using a BCA Protein Assay Kit (Pierce™, ThermoFisher). The

Invitrogen Mini Gel Tank, the iBlot 2 Dry Blotting System, and the iBind Western Systems were used for protein gel electrophoresis. The SuperSignal™ West Pico PLUS Chemiluminescent Substrate (ThermoFisher) was used to visualize the protein level.

Chromatin Immunoprecipitation (ChIP) Assay

ChIP assay was carried out using the iDeal ChIP-qPCR Kit (Diagenode) according to the manufacturer's protocol. Rabbit anti-FOXO1 (Abcam) and IgG from the kit were used to detect FOXO1 specific binding on the chromatin. Quantitative PCR was performed using PowerTrack SYBR Green Master Mix (ThermoFisher). The primer sequences for FOXC2 promoter -0.3kb area are: 5' TGTCCCAGGATCATTGCTACT 3' (forward) and 5' ATTTTGGTGAATGGGCCCAC 3' (reverse); for -1.4kb area is: 5' GCCCGTGTTTAGCCTTGTTA 3' (forward) and 5' TAGGAATCCCGGACAGTTTG 3' (reverse); for -2.7kb area is: 5' TTAGGCTTTATCGCCGCTTA 3' (forward) and 5' TTTTCCCCCTTCTTGACCTT 3' (reverse).

Vessel Isolation and Cannulation

Mice were anesthetized by intraperitoneal injection of ketamine/xylazine (100/10 mg/kg) and placed in the prone position on a heated tissue dissection/isolation pad. A midline abdominal incision was made so that the entire small intestine could be exteriorized. The intestine was then cut at the duodenum and cecum, rinsed in Krebs solution and pinned to a Sylgard platform. Mesenteric collecting lymphatic vessels were identified and removed. These were then pinned to the bottom of a dissection chamber for removal of excess fat and connective tissue. A cleaned lymphatic vessel was then transferred to a 3-ml observation chamber containing Krebs-albumin solution and cannulated at each end with a glass micropipette (40-50 um OD tip) and pressurized to 3 cmH_2O. The same pair of cannulation pipettes was used for all experiments. The chamber, mounted on a platform with attached micropipettes, pipette holders and micromanipulators was transferred to the stage of an inverted microscope. Polyethylene tubing connected the back of each micropipette to low-pressure transducers and a computerized pressure controller (6). To minimize longitudinal bowing at higher intraluminal pressures, input and output pressures were

briefly set to 10 cmH_2O at the beginning of every experiment, and the vessel segment was stretched axially to remove longitudinal slack. With both pressures set to 3 cmH_2O, the vessel was allowed to equilibrate in Ca^{2+}-free Krebs buffer at 37°C for at least 20 min to eliminate spontaneous contractions that otherwise would have interfered with valve function tests. Constant exchange of buffer was maintained using a peristaltic pump at a rate of 0.5 mL/min. Custom LabVIEW programs (National Instruments; Austin, TX) acquired real-time analog data from the pressure transducers simultaneously with vessel inner diameter, as detected from video images acquired at 30-40 fps using a Basler A641fm firewire camera (74). Digital videos of the valve function protocols, with embedded pressure data, were recorded for off-line analyses.

Valve Function Tests

All lymphatic segments used for these protocols contained a single valve. Luminal pressure on the inflow side of the valve was measured with a servo-null micropipette inserted through the wall; an initial hole was made with a pilot pipette, which was then removed and replaced with the servo-null pipette. The latter was advanced to seal the hole. The calibration of the servo-null pipette was checked, and adjusted as needed, by raising and lowering inflow pressure (Pin) and outflow pressure (Pout), simultaneously, between 0.5 and 10 cmH_2O.

To ensure accurate and consistent measurements, 1) all three transducers were calibrated before each experiment; 2) the same pair of cannulation pipettes (i.e. with fixed resistances) was used for all experiments; 3) the pipettes were cleaned after each experiment and checked before each valve test to ensure that the pipette tips were free of debris; 4) the lines were free of bubbles; 5) the Psn pipette calibration was rechecked at the end of the valve test.

The first test measured pressure back-leak through the closed valve. Starting with inflow pressure (Pin) and outflow pressure (Pout) = 0.5 cmH_2O, and the valve open, Pout was raised, ramp-wise, to 10 cmH_2O over ~1 min period while Pin was held at 0.5 cmH_2O. Normal valves closed as Pout exceeded ~1 cmH_2O and remained closed for the duration of the Pout ramp. Pressure back-leak

through the closed valve was measured using the servo-null micropipette, which had a resolution of ~0.05 cmH_2O. The value of servo-null pressure (Psn) at Pout = 10 cmH_2O was used as a standard index of back-leak; however, additional values of Psn at intermediate Pout levels were determined offline using a LabView program by binning the Pout data in 1 cmH_2O intervals. Pressure back-leak was calculated from (Psn-Pin).

The second test measured pressure back-leak through a closed valve when Pout was varied from 10 to 100 cmH_2O in steps of 10 cmH_2O. Although these pressures are supra-physiological for mice, the high Pout levels potentially could uncover and amplify subtle degrees of back-leak that otherwise would be difficult to detect at Pout levels from 0.5 -10 cmH_2O. This test was performed starting at Pin=Pout=0.5cmH_2O and raising Pout ramp-wise to 10 cmH_2O. A valve on the outflow line was then turned to connect the Pout pipette to a manually adjustable reservoir and the reservoir was elevated in steps of 10 cmH_2O from 10 to 100 cmH_2O while measuring Psn upstream from the closed valve. Pressure back-leak was calculated from (Psn-Pin). Pout levels typically were not monitored by the pressure transducers during this test because the higher levels exceed the overpressure range of the sensor elements.